CrossMark

ORIGINAL PAPER

Experimental Research on Characteristics of Fault Activation and Confined Water Rising

Guangli Zhu · Wenquan Zhang · Shuli Wang · Peisen Zhang

Abstract Water inrush due to fault activation in deep coal mining is the main type of water disaster in central and eastern China. This paper analyzed the primary form and mechanism of fault activation that triggers water inrush and derived the critical conditions for fault activation. The WuGou coal mine is used as a geological example, and the characteristics of the fault activation and mechanism of the confined water rising were researched by similar simulation experiments. The results provide the following conclusions. (1) There are three forms of fault activation that trigger water inrush: continuous fault, hidden fault and associated fault activation. (2) Mining causes high abutment pressure in a coal seam; this pressure transfers to the floor, causing damage and failure. The maximum failure depth occurs when the overlying strata is in a critical fractured state. The cracks of the floor gradually close in the goaf. (3) The fault activation causes water inrush and exhibits four stages: fault zone yielding caused by high stress, cracking and extending of the fault zone, movement and slippage of the fault zone, and confined water rising. (4) The influence factors of the confined water rising were analyzed. The experimental results show a negative correlation between the confined water height and distance to the fault zone and a positive correlation among the confined water pressure, fault zone width and confined water height. In addition, a strong–weak–strong change law of the confined water pressure with height is observed.

Keywords Fault activation · Similarity simulation experiment · Floor failure · Confined water rising

1 Introduction

Coal mining activities triggering confined water inrush is the main type of water disaster in deep mining projects in China, and fault activation caused by mining-induced water inrush accounts for 80% of the water disasters (Li and Fu 2006). With resource depletion, mining depths are increasing; which worsens the mining conditions and increases the ground pressure and confined water pressure (which reaches 10 MPa in some deep mining areas), increasing the risk of confined water inrush (Gui and Lin 2016). To achieve safe and efficient mining of deep coal resources, it is important to determine the characteristics of fault activation and mechanism of confined water rise.

G. Zhu (✉) · W. Zhang · P. Zhang
College of Mining and Safety Engineering, Shandong University of Science and Technology, Qingdao 266590, China
e-mail: zhugli8910@163.com

S. Wang
Resources and Environmental Engineering, Shandong University of Technology, Zibo 255000, China

In the last decade, many scholars have researched the mechanisms of fault activation and water inrush, influencing factors, and prediction and control technologies by using different methods and means, such as theoretical derivation, numerical simulation and laboratory experimentation. The critical conditions for the fault dip angle, mining depth, and mining distance have been calculated and derived from Mohr–coulomb failure criteria (Shi and Hou 2011). The maximum critical pressure of confined water has been calculated (Lu et al. 2014). The influence factors of fault activation, the movement and failure state of the overlying strata, and the failure process of the floor have been studied by using the numerical simulation software FLAC, COMSOL, and RFPA (Li et al. 2009; Zhang et al. 2016; Liu and Wu 2008). The failure process, penetrability, critical water pressure, and distribution of stress in small rock samples have been tested in the laboratory by different experimental methods (Qiao et al. 2013). The mechanism driving prediction methods and control technologies of fault-activation-induced water inrush has been proposed (Song et al. 2013). With the development of microseismic monitoring technology, precursor information and characteristics of water inrush have been analyzed, and have provided new ways to predict water inrush. Scholars have researched other aspects of fault-activation-induced confined water inrush through different methods (Sun and Wang 2013).

This paper studies the characteristics of fault activation and the mechanism of confined water rise by using large similar simulation tests. In these tests, the facilities and equipment were independently designed. Then, the floor failure, fault activation characteristics, mechanism of confined water rise and influence factors are analyzed.

2 Form and Critical Conditions of Confined Water Inrush by Fault Activation
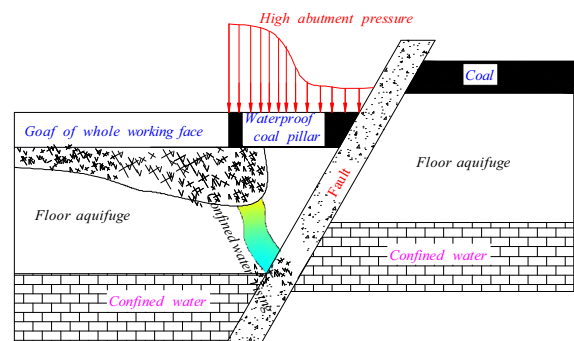
2.1 Form of Water Inrush by Fault Activation

The formation conditions of strata and later geotectonic movement cause numerous fault structures in natural strata. Fault structures create discontinuities in the initial strata, which naturally include weak interlayers. Deep mining causes high abutment pressure, creating a large and deep failure zone within the floor;

faults can also be activated during mining activities. Finally, confined water rises along these activated fault zones in the damaged floor area and then suddenly inrushes into the working face, causing a water disaster. The fault activation that induces confined water inrush can be divided into three forms: continuous fault, hidden fault and associated fault activation (Chen et al. 2011).

2.1.1 Continuous Fault Activation Triggering Water Inrush

Continuous faults are the most common fault structures under natural geological conditions and are the most threatening geological structures in mining activities. Continuous faults offset initially continuous strata and coal seams, and mining the upper plate of a reverse fault reduces the distance from the coal seam to the confined water layer (Tang et al. 2011).

In most mining activities, continuous fault activation triggering confined water inrush shows a clear characteristic of a time delay, and most events occur in the goaf, which is mined over and closed. Keeping a large waterproof pillar along the fault zone in shallow mining can effectively prevent fault activation. However, this is not infeasible in deep mining. In deep mining, the high abutment pressure of the goaf transfers to the waterproof pillar, forming a high stress concentration; increasing the stress over a critical limit, causing the fault zone to yield, fracture development, extension, and structural variation. Finally, a confined water inrush occurs along the fractures in the waterproof pillar and floor, causing a water disaster. The first water inrush location is the junction of the waterproof pillar and failure floor of goaf, as shown in Fig. 1 (Li et al. 2011).

Fig. 1 Continuous fault activation triggering water inrush

2.1.2 Hidden Fault Activation Triggering Water Inrush

Hidden faults are small fault structures that offset continuous strata within a limited range; hidden faults have limited extensions and are difficult to identify. Therefore, hidden faults are the most easily ignored fault structure in mining activities. Numerous engineering practices have shown that the confined water inrush due to hidden fault activation is more instantaneity and unpredictable (Han et al. 2009).

Hidden fault activation often triggers confined water inrush during working face mining. During coal mining, the load of the overlying strata transfers to the floor through the coal seam, causing floor damage and fracture development; simultaneously, the lower hidden faults are also activated. Once the floor fractures extended to the hidden fault, the confined water suddenly bursts into the mining working face, creating a water disaster, as shown in Fig. 2.

2.1.3 Associated Fault Activation Triggering Water Inrush

During the formation of large and continuous fault structures, many associated small faults are often formed in the vicinity; these associated faults clearly have limited extensions and are difficult to identify. In mining activities, we often attach considerable importance to large fault structures and easily ignore the associated faults; therefore, associated fault activation

can suddenly and unpredictably conduct water burst into the working face.

Associated fault activation generally triggers water inrush near the stop line of the mining working face. When designing waterproof pillars, we tend to consider the geological conditions of large faults and ignore that the associated faults may extend outside of the waterproof pillars. Near the mining stop line, the associated faults activate because of the high abutment pressure on the waterproof pillar (Wang et al. 2016). In addition, when the associated faults connect with the fractures in the floor, confined water burst into the working face can occur instantly, as shown in Fig. 3.

2.2 Critical Conditions of Fault Activation

Based on classical fault theory (Yin et al. 2015) and mining activities, a mechanical model of fault activation is established, as shown in Fig. 4. In Fig. 4, AB is the fault plane; σ_x and σ_y are the horizontal and vertical stresses acting on the fault, MPa; P is the pressure of the confined water on the fault plane, MPa; and α is the dip angle of the fault.

The normal stress on the fault plane:

$$\sigma_n = \frac{\sigma_z + \sigma_x}{2} + \frac{\sigma_z - \sigma_x}{2}\cos 2\alpha - p \tag{1}$$

The shear stress on the fault plane:

$$\tau_n = \frac{\sigma_z - \sigma_x}{2}\sin 2\alpha \tag{2}$$

According to the Mohr–coulomb failure criterion, the shear strength of the fault plane:

$$\tau_f = c + \sigma_n \tan \varphi \tag{3}$$

where c is the cohesion of the rock, MPa, and φ is the internal frictional angle.
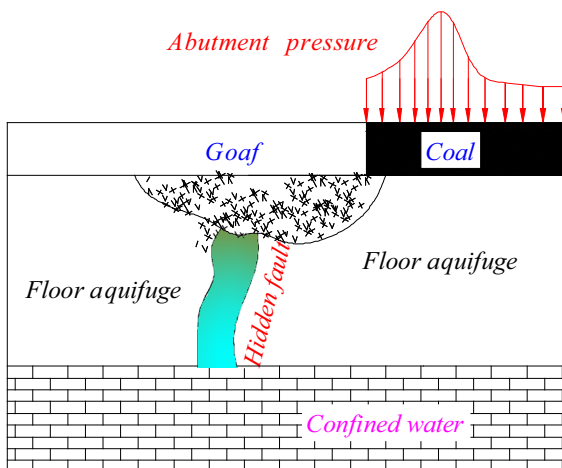

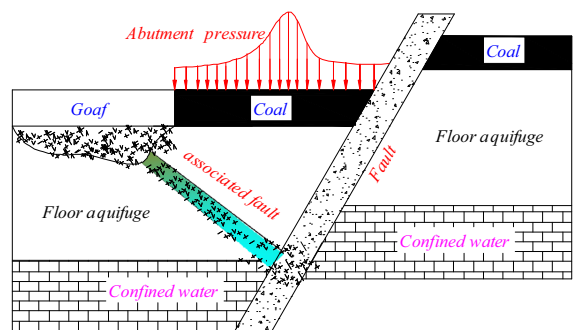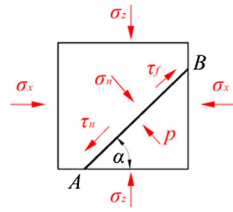**Fig. 2** Hidden fault activation triggering water inrush

Fig. 3 Associated fault activation triggering water inrush

Fig. 4 Mechanical model of fault activation

Many engineering practices and experiments have shown that fault activation is shear failure. Thus, the critical condition of fault failure is $\tau_n \geq \tau_f$.

$$\tau_n \geq c + \sigma_n \tan \varphi \tag{4}$$

With formulas (1), (2) and (4), the critical pressure of the confined water can be written as follows:

$$P = \frac{\sigma_z + \sigma_x}{2} + \frac{\sigma_z - \sigma_x}{2} \cos 2\alpha + \frac{2c - (\sigma_z - \sigma_x) \sin 2\alpha}{2 \tan \varphi} \tag{5}$$

According to the basic theory of mining ground pressure (Huang 2007):

$$\begin{cases} \sigma_z = K\gamma H \\ \sigma_x = \lambda \sigma_z = \lambda K\gamma H \end{cases} \tag{6}$$

where K is the maximum stress concentration factor; γ is the unit weight of the overlying strata, kN/m^3; H is the mining depth, m; and λ is the lateral pressure coefficient.

From formulas (5) and (6):

$$P = \frac{K\gamma H(1 + \lambda)}{2} + \frac{K\gamma H(1 - \lambda)}{2} \cos 2\alpha + \frac{2c - K\gamma H(1 - \lambda) \sin 2\alpha}{2 \tan \varphi} \tag{7}$$

Formula (7) is the formula used to calculate the critical pressure of the confined water due to the fault activation. In engineering practices, if the practical pressure of the confined water is greater than this critical pressure, the fault can be activated; otherwise, the fault cannot be activated (Sun et al. 2015).

Transforming formula (7):

$$H = \frac{1}{K\gamma} \times \frac{2c - 2P \tan \varphi}{(1 + \lambda) \sin 2\alpha - [(1 + \lambda) + (1 - \lambda) \cos \alpha] \tan \varphi} \tag{8}$$

Formula (8) is the calculated formula of the critical mining depth. In engineering practices, if the practical mining depth is deeper than this critical depth, the fault can be activated; otherwise, the fault cannot be activated (Wu et al. 2004).

3 Experimental Fault Activation

3.1 Experimental Equipment

Based on a two-dimensional similar simulation test bed, we designed and modified equipment for testing, as shown in Fig. 5, including the two-dimensional similar simulation test bed, confined water loading system, floor aquifuge system and confined water rising system.

3.1.1 Two-Dimensional Similar Simulation Test Bed

The two-dimensional similar simulation test bed, which mainly includes a frame and hydraulic jacks, is used to create and simulate the faults and adjacent strata. The dimensions of the similar simulation test bed are length × width × height of 3 × 0.4 × 1.8 m (where 1.8 m is the effective height of the model).

3.1.2 Confined Water Loading System

The confined water loading system includes water supply and return pipes. The water supply pipe is attached to a pressure pump, pressure tank, one-way valve, pressure governing valve and manometer. The pressure pump can pressurize water in the pressure tank to provide an initial water pressure. The one-way valve can prevent water return to the pressure tank when the water pressure is insufficient. The governing valve and manometer can control the accuracy and continuity of the water pressure in the water bag. The return pipe is attached to a pressure relief valve, manometer, one-way valve and return tank. The pressure relief valve and manometer can effectively guarantee the stability of the water pressure in the water bag and can self-regulate when the water bag pressure exceeds a critical limit. The return tank can recover the water from the water bag for recycling.
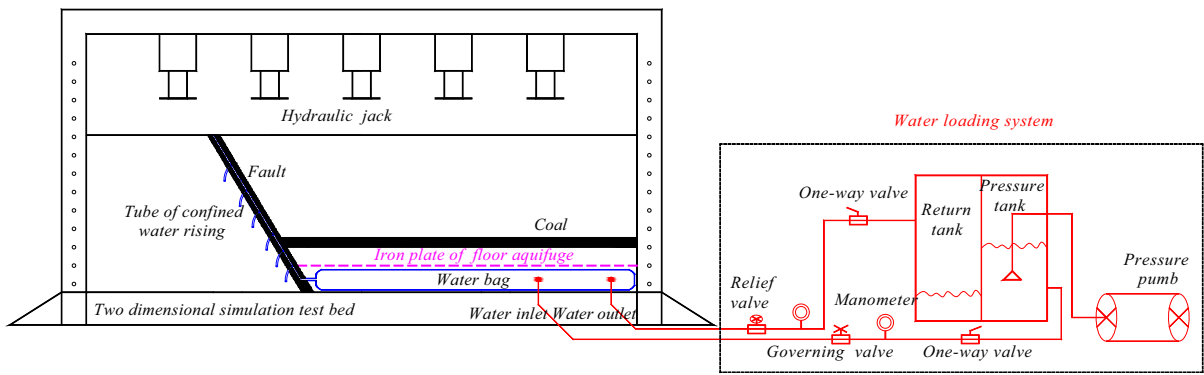
Fig. 5 The experimental system to study fault activation triggering confined water inrush

3.1.3 Floor Aquifuge

The floor aquifuge is a Q235 iron steel plate. The dimensions of the iron plate are length × width × thickness of $40 \times 10 \times 0.5$ cm. A certain distance between two plates (1–2 cm) is created to simulate the fractured floor, which was damaged by high stress.

3.1.4 Confined Water Rising System

The confined water rising system is mainly composed of a water bag, confined water rising tube and drainage tube. The water bag is mainly made of rubber with a good flexibility and ductility, which is customized. The dimensions of the water bag are width × height of 40×14 cm; 40 cm is the test bed width, 14 cm is the height of the single iron protecting plate of the similar simulation test bed, and the length of the water bag is adjustable. The confined water rising tube is soft and black, with a diameter of 2 cm. The drainage tube is a typical medical infusion tube, connecting to the confined water rising tube across a certain distance (2–5 cm). Each drainage tube is equipped with a control valve. When the confined water rises along the rising tube to the drainage tube, the water may be spilled.

3.2 Engineering Background

The WuGou coal mine is in the LinHuan mining area of the HuaiBei coalfield in China. There are 7 fault structures with fault throws greater than 100 m in the mining area. The widths of the fracture zone of the faults are 2–60 m; these zones are mostly filled with mudstone, with lesser amounts of siltstone and sandstone. No water leakage occurred during the site drilling; therefore, these faults are non-water-conducting faults. At present, the mining coal seam is the tenth in the central part of the Shanxi Formation and has an average thickness of 3.94 m. The rock within 30 m of the roof is mainly a medium-grained sand and siltstone. The average distance from the coal seam to the confined water (Taiyuan formation) is 41.9 m. The rock in this area is mainly interlayered siltstone, sandstone and mudstone.

The experiment uses the tenth coal seam, which is mined in the No. 1033 working face at a depth of 400–550 m, as an example. The F13 fault extends 5.2 km and is close to the ventilation roadway; the throw of this fault is 100–240 m. For the F13 fault, the main water inrush threat is from the water in the Taiyuan limestone, which this fault offsets (confined water pressure of 3.2 MPa). The location and layout of the working face is shown in Fig. 6.
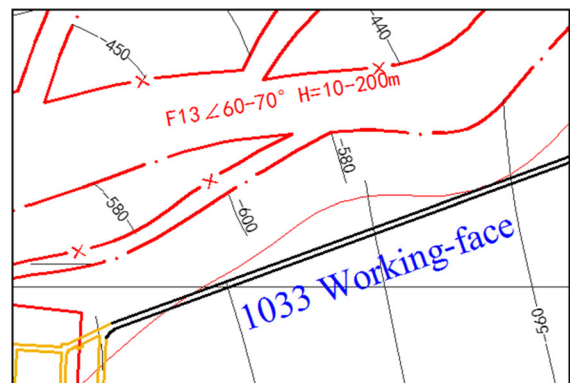
Fig. 6 Layout of the working face and fault F13 (unit: m)

3.3 Test Parameters and Process

3.3.1 Parameters

The fault dip angle is 70°, the fault throw is 148 m, and the thickness of the coal seam is 4 m. The distance from the coal floor to the confined water is 42 m. The coal seam and strata are horizontal. We mainly study the overlying strata movement and floor failure: 100 m from the upper plate to the coal seam and 40 m from the coal seam to the confined water. According to the parameters measured from the engineering background and the theory of similarity simulation experiments (Lu and Wang 2015), the geometrical similarity is 1:100, and the strength similarity is 1:150.

Therefore, the experimental confined water pressure is 21 kPa. According to the similar materials used by other scholars, we used river sand as the aggregate material, and calcium carbonate and gypsum as the cementing materials (Yuan et al. 2015; Zhu et al. 2017). In the upper boundary of model loads compensating stress 65 kPa. By testing specimens composed of similar materials, we determined the ratio of the similar materials. The parameters used to create the strata layers and to determine the weight of each material is shown in Table 1.

To study the influence of the width of the fault zone on the confined water rising, we designed different widths of the fault zone (1, 2 and 4 cm) along the direction of the test bed; the faults were placed at 10, 20 and 10. The fault zone is filled with a mixture of mica and mudstone and is lightly compacted when laid. To reflect the instantaneous confined water height, the tube of the confined water rising is connected with the drainage tube at different heights, and the drainage tube drains to the surface of the experimental model. Below the coal seam and along the fault zone, drainage pipe is set every 2 cm; the drainage pipe is set every 4 cm above the coal seam. To monitor the abutment pressure and floor stress, especially the stress variation in the fault zone, stress sensors are added in the model. The parameters of the experimental model are shown in Fig. 7.

3.3.2 Experimental Process

According to the test scheme and parameters, the following experimental setup was performed: laying the upper and lower plates of the fault strata, assembling the confined water loading system, and installing the stress sensors and iron plates. After the strata were added, a 10 × 10 cm grid was drawn on the front surface of model. The coal seam was excavated incrementally (5 cm), to 30 cm from the fault zone; data were collected on the confined water height, stress sensor changes, and observations of the fracture development in the floor. During coal seam mining, the change in the confined water pressure was kept within a certain range (10 kPa), and the drainage from the drainage tube was recorded to study the law of confined water rising with pressure change.

4 Experimental Results

4.1 Floor Failure Mechanism

As the working face is mined, the abutment pressure in the coal body gradually increases. When the working face advances to 30 cm, the stress at measuring point 4 is 240 kPa, which is twice the original pressure. According to the distribution of the abutment pressure, the range of influence of the mining activities is 30 cm. The changes in stress at measuring point 4 are shown in Fig. 8.
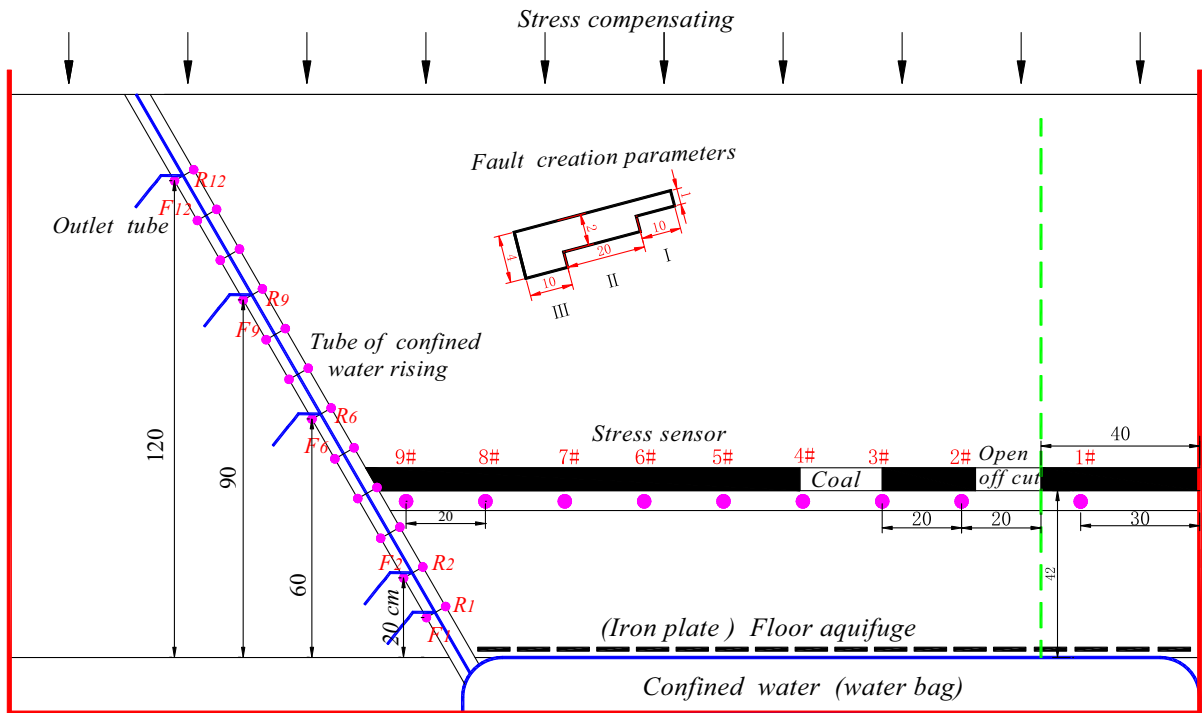
The high abutment pressure transferring to the floor creates a stress concentration in the strata of the floor, and the stress increases gradually. As the abutment pressure decreases rapidly in the goaf and the confined water pressure remains high, the iron plates begin to rise (Fig. 9a). Finally, the fractures in the floor form and extend gradually (Fig. 9b). Before the first movement of the overlying strata (40 cm), the depth of the floor failure and fracture development reaches a maximum 13–15 cm (Fig. 9c). With continued mining, the overlying strata breaks and compacts in the goaf, causing the floor fractures to gradually close (Fig. 9d). The floor strata periodically exhibit failure processes.

### 4.2 Characteristics of Fault Activation

Taking the distance from the coal wall to the fault zone as a reference, the mining activity-induced fault activation can be divided into four stages: fault zone yielding caused by high stress, cracking and extending

Table 1 The mixture ratios of the similar materials and the components of each layer

Number	Thickness/cm	Ratio	Length/cm	Weight/kg			
				Sand	Calcium carbonate	Gypsum	Water
R12	10.4	7:5:5	271.14	43.43	2.58	2.58	3.31
R11	20.0	8:6:4	264.04	61.96	3.87	2.58	4.66
R10	1.2	8:6:4	252.49	17.78	1.11	0.74	1.30
R9	6.0	8:6:4	251.80	44.32	2.77	1.85	3.33
R8	2.4	8:6:4	248.34	34.97	2.62	1.75	3.93
R7	13.2	8:6:4	246.95	31.87	2.00	1.30	2.40
R6	6.0	7:8:2	239.33	44.23	4.20	1.00	3.50
R5	10.0	8:6:4	235.87	34.59	2.16	1.44	2.60
R4	6.6	7:5:5	230.09	31.18	1.86	1.86	2.34
R3	6.2	8:6:4	226.28	41.15	2.50	1.72	3.80
R2	5.7	7:8:2	222.53	39.07	3.72	1.04	4.08
R1	12.0	7:7:3	219.24	40.52	3.38	1.45	3.70
M	4.0	8:6:4	212.31	24.91	1.56	1.05	2.24
F1	5.0	7:5:5	210.00	32.34	1.93	1.93	3.00
F2	2.2	8:6:4	207.11	26.73	1.67	1.12	2.41
F3	10.4	7:5:5	205.84	32.97	2.35	2.35	3.01
F4	2.4	8:6:4	199.84	28.11	2.11	1.40	2.50
F5	4.0	8:6:4	198.45	23.29	1.75	1.16	2.10

Number	Thickness/cm	Ratio	Length/cm	Weight/kg			
				Sand	Calcium carbonate	Gypsum	Water
F6	18.0	7:5:5	196.41	36.25	2.59	2.59	3.31
F7	18.0	7:5:5	39.42	7.29	0.43	0.43	0.55
F8	4.0	7:6:4	41.73	10.28	0.73	0.48	0.78
F9	2.0	8:6:4	42.89	5.03	0.32	0.21	0.38
F10	6.0	7:6:4	46.35	8.57	0.66	0.40	0.78
F11	3.6	8:6:4	48.43	10.22	0.63	0.43	0.77
F12	12.0	7:6:4	55.36	10.23	0.73	0.48	0.80
F13	4.50	7:5:5	57.96	16.06	0.95	0.95	1.23
F14	5.0	8:6:4	60.84	8.92	0.67	0.45	0.70
F15	12.0	7:6:4	67.77	25.05	2.15	1.43	2.20
F16	2.4	8:6:4	69.16	9.74	0.73	0.49	1.10
F17	2.0	7:6:4	70.31	8.66	0.62	0.41	0.70
F18	18.0	8:6:4	80.71	14.20	0.90	0.90	1.30
F19	6.0	7:6:4	85.61	20.10	1.75	1.16	2.10
F20	13.5	8:6:4	93.46	24.80	1.86	1.24	2.80
F21	18.0	7:6:4	103.86	19.19	1.65	1.10	2.19
F22	18.0	8:6:4	114.25	20.11	1.51	1.01	2.26

Fig. 7 Experimental parameters (unit: cm)
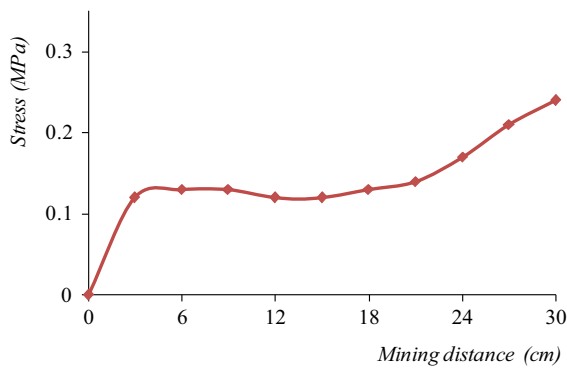
Fig. 8 Stress change law at measuring point 4

of the fault zone, movement and slippage of the fault zone, and confined water rising (Miao et al. 2011).

### 4.2.1 Fault Zone Yielding Caused by High Stress

When the working face advanced 50–55 cm to the fault zone (Fig. 10a), the pressure on both sides of the fault zone under the coal seam clearly increased. The maximum pressure at point F2 and R2 were 240 and 280 kPa, considerably higher than the compressive strength of the fault zone filling, causing yielding of

the fault zone filling (the fault zone filling compressive strength is 100 kPa). The mixture of mica and mudstone used to fill the fault zone was extruded to the surface of the model. Due to the compressive deformation of the coal seam near the fault zone, and large section of overlying strata lost stability and rotated, causing the fault zone above the coal seam to clearly experience tension and shear. Finally, the filling of the fault zone yielded and failed, clearly exhibiting extension, and the phenomenon of micro-fracture development occurred (Fig. 10b).

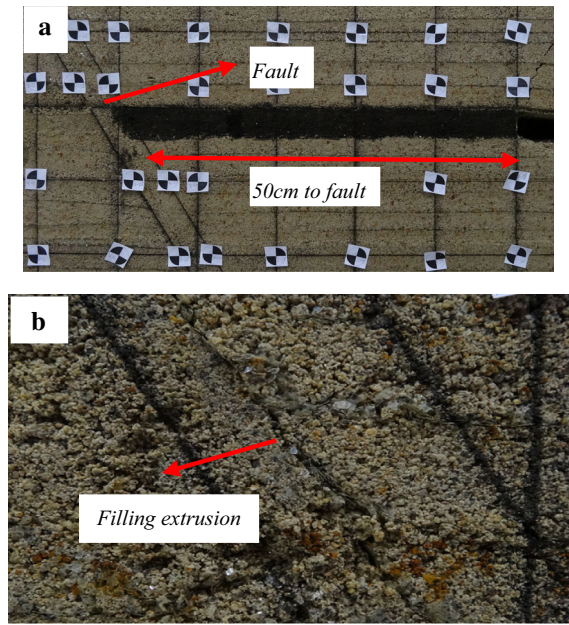### 4.2.2 Cracking and Extending of the Fault Zone

When the working face advanced 40 cm to fault zone (Fig. 11a), due to the thick overlying strata, the upper plate rotated and subsided, and the micro-fractures in the fault zone above the coal seam stretched and extended to form macro-fractures and a small number of through going cracks. Simultaneously, due to high abutment pressure, the coal body was further compressed, and the upper fault zone plate showed a clear settlement. The highest stress was 390 and 470 kPa at points F2 and R2, and the fault zone was further
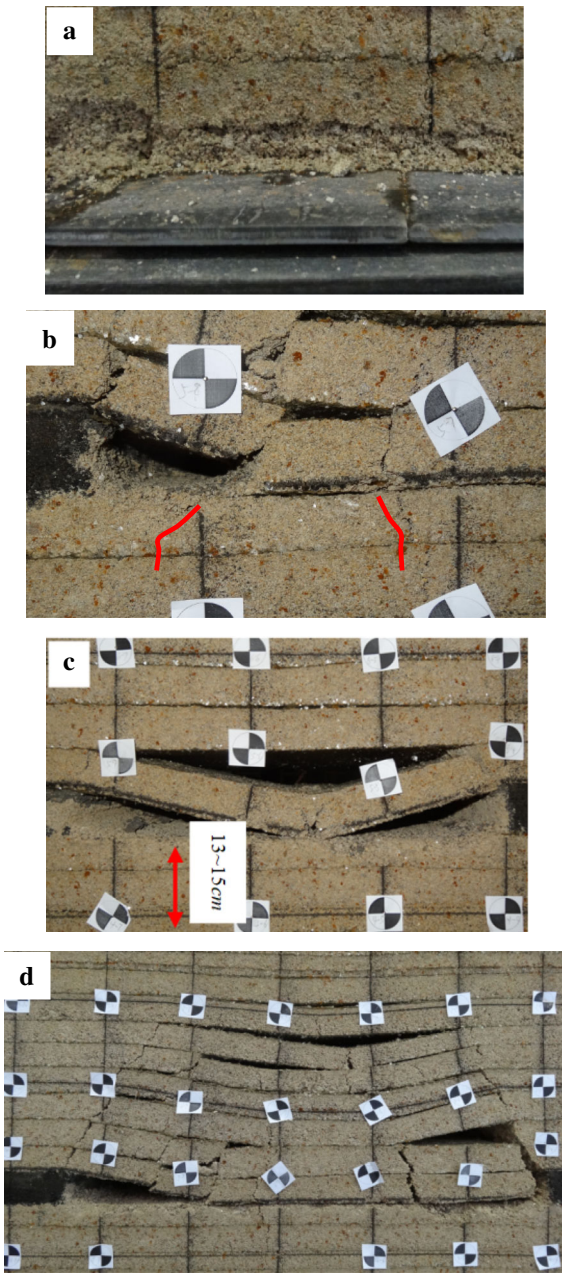
Fig. 9 The failure process of the floor. **a** Iron plates rising. **b** Fracture development. **c** The maximum depth of fracturing. **d** Floor fractures closed in the goaf

compressed and destroyed. Fractures and cracks developed and extended in the floor next to the coal wall, due to undergoing shear and high abutment and confined water pressures. While the stored energy and stress of the fault released, the highest stress peak was transferred to the coal seam away from the fault zone.

Fig. 10 Fault zone yielding caused by high stress. **a** Distance to the fault zone. **b** Micro-fracture development
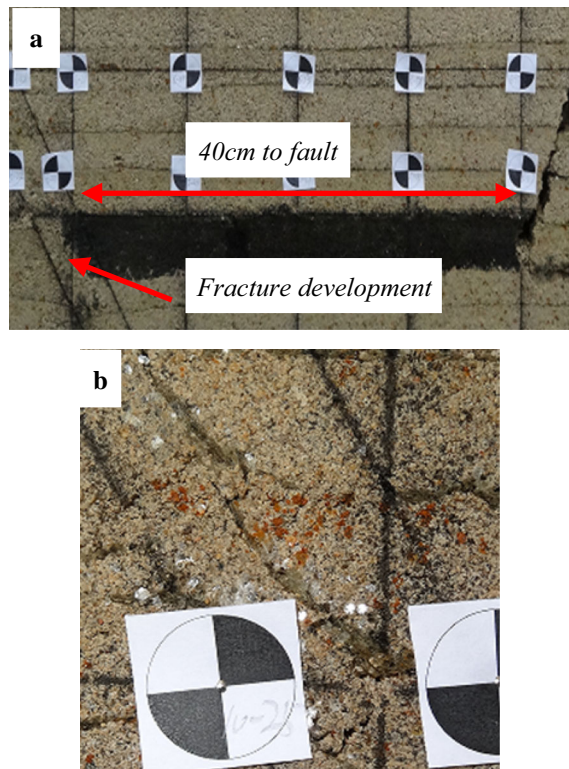
Fig. 11 Cracking and extending of the fault zone. **a** Distance to the fault zone. **b** Cracks extending

Due to the abutment pressure and confined water pressure, the macro-fractures and cracks in the fault zone begin to propagate through the strata, as shown in Fig. 11b.
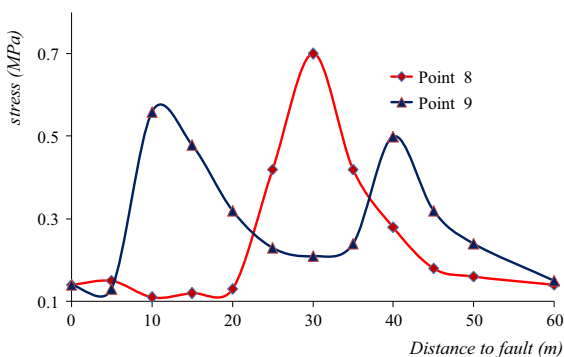
4.2.3 Movement and Slippage of the Fault Zone

When the working face advanced 30 cm to fault zone (Fig. 13a), the cracks in the fault zone in the upper coal seam were exacerbated, and their opening gradually increased from bottom to top. The upper plate slides downward, and the two fault plates clearly move. The stress in the coal body 15–20 cm from the fault zone quickly increased; the stress of measuring point 8 (5 cm from the coal wall) is 700 kPa (super-imposed by the peak abutment pressure and tectonic stress). Simultaneously, the stress in the coal body near the fault zone quickly decreased; the stress of measuring point 9 (5 cm from the fault zone) is 700 kPa, greater than the initial stress at this point. Under tectonic stress, the stress curve has a double peak, as shown in Fig. 12.
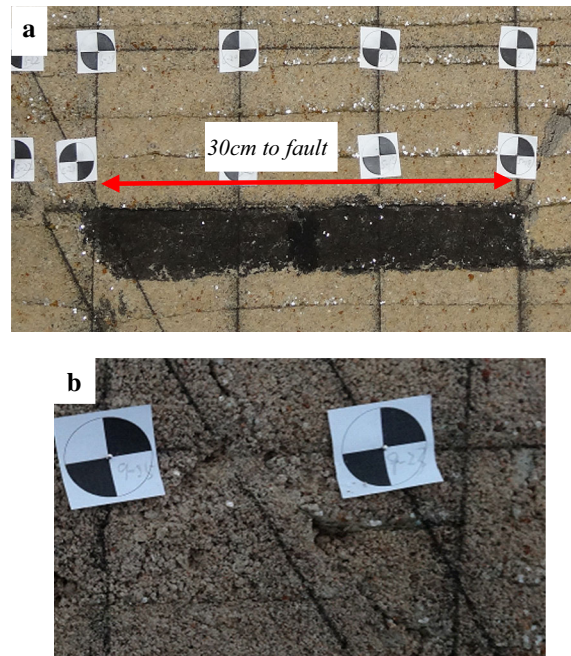
Therefore, a large stress difference is generated between the coal wall and fault zone; combined with the effect of the confined water, the floor near the coal wall and the fault zone will become damaged due to the development and propagation of cracks, especially cracks through the floor and fault zone, as shown in Fig. 13b.

4.2.4 Confined Water Rising

As the fractures extend farther, major and through going cracks form in the fault zone above coal seam and floor. Although there are no completely through

Fig. 13 Movement and slippage of the fault zone. **a** Distance to the fault zone. **b** Slippage of the fault zone

going cracks in the fault zone below the coal seam, the development of macro-cracks possibly causes water to rise, especially since there are cracks that cut through the floor and fault zone. Once the confined water pressure reaches the required condition (later measured to be 15 kPa), or with the long-term effect of confined water, fault activation and water rising may occur, as shown in Fig. 14. During mining of the remaining the coal pillar (30 cm), the drainage tubes drain water; then, when excavating 20–25 cm from the fault zone, the confined water rises and drains quickly. The height of the confined water level decreases and remains stable after mining through the fault zone (Zhang et al. 2013).

Fig. 12 The stress curves of points 8 and 9

Fig. 14 The throughgoing fracture on the surface of the fault zone
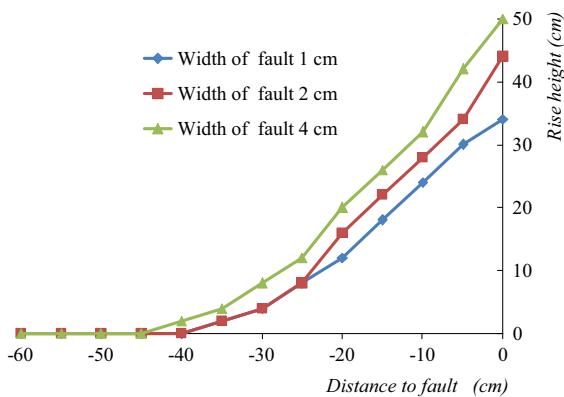
4.3 Influence Factors of Confined Water Rising

By controlling and changing the pressure of the confined water, distance between the fault zone and coal wall, and width of the fault zone, we quantitatively studied the influencing factors of confined water rising due to fault activation, based on the height of the confined water rise along the fault zone (Zhu et al. 2009; Wang et al. 2015).
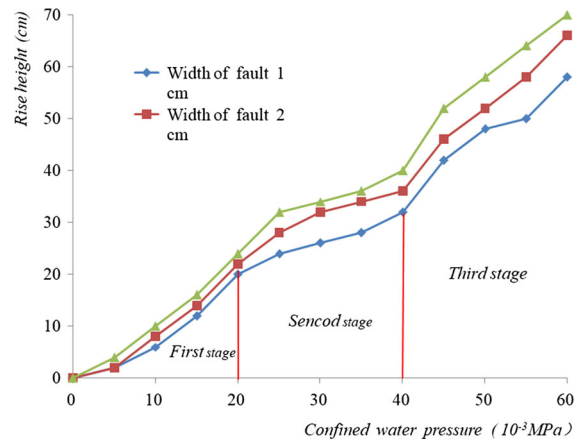
Keeping the confined water pressure at a constant 20 kPa, we observed the rising confined water level at different distances (from the coal wall to the fault zone), as shown in Fig. 15. The results show that there is a negative linear correlation between the water level and distance. When the distance is 40–45 cm, the confined water starts to rise along the fault zone; then, the fault starts to activate and conduct water. Confined water rises quickly at the three different fault zone widths, especially when the distance to the fault is 20–25 cm.

When the distance is 25 cm (from the coal wall to the fault zone), the greatest quantitative change in the confined water pressure is 3 times the original water pressure (20 kPa). The correlation curve of the confined water height and pressure is shown in Fig. 16 and has a positive correlation. The curve can be divided into three stages, and shows a strong–weak-strong trend. Especially when the pressure exceeds 40 kPa, the confined water rises rapidly because of the high-pressure confined water, and the water height exceeds 40 cm (coal seam position), suggesting that the fault zone above the coal seam is more active than that below the coal seam.

The conclusion that can be drawn from Figs. 15 and 16 is that there is a positive correlation between the

Fig. 16 The correlation curve between the height and pressure of the confined water

width of the fault zone and confined water height, at the same distance and water pressure. In the early stage, the correlation was weak, but the correlation gradually increased with the decrease in the distance to the fault and increase in confined water pressure (Peng et al. 2013; Shi et al. 2012).

5 Conclusions

1. There are three forms of fault activation that trigger water inrush: continuous fault, hidden fault and associated fault activation. Continuous fault activation triggering water inrush is a common water disaster and mostly occurs in the goaf at the end of mining activities, and the first water inrush location is the junction of the waterproof pillar and failure floor of goaf. Hidden fault activation triggering water inrush often occurs during working face mining, and these events are sudden and unpredictable. Associated fault activation triggering water inrush generally occurs near the stop line of the mining working face, these events are often not observed and can be ignored.

2. Mining activities causes high abutment pressure in the coal body; this pressure is transferred to the floor, causing floor failure and damage. The maximum failure depth is generated when the overlying strata are in a critical fractured state and the cracks of the floor gradually close in the goaf. The failure of the floor is a periodic process.

Fig. 15 The correlation curve between the confined water height and distance from the coal wall to the fault zone

3. The fault activation that triggers water inrush exhibits four stages: fault zone yielding caused by high stress, cracking and extending of the fault zone, movement and slippage of the fault zone, and confined water rising. The fault zone above the coal seam yields under tension and shear, and the fault zone below the coal seam yields under compression. The fault zone below the coal seam activates after the fault zone above the coal seam.

4. There is a negative correlation between the confined water height and distance to the fault zone, and there is a positive correlation between the confined water pressure, fault width and confined water rising height. In addition, a strong–weak-strong change law between the confined water pressure and height was observed; in the early stage, the correlation is weak, but the correlation gradually increased with the decrease in the distance to the fault zone and increase in the confined water pressure.

References

Chen ZH, Hu ZP, Li H et al (2011) Fracture mechanical model and criteria of insidious fault water inrush in coal mines. J China Univ Min Tech 40(5):673–677

Gui H, Lin M (2016) Types of water hazards in China coal mines and regional characteristics. Nat Hazards 84:1501–1512

Han J, Shi LQ, Yu XG et al (2009) Mechanism of mine water inrush through a fault from the floor. Min Sci Technol 19:276–281

Huang QX (2007) Experimental research of overburden movement and subsurface water seeping in shallow seam mining. J Univ Sci Technol Beijing Miner Metall Mater (Eng Ed) 14(6):483–489

Li HM, Fu K (2006) Some major technical problems and counter measures for deep mining. J Min Saf Eng 23(4):468–471

Li LC, Tang CA, Liang ZZ et al (2009) Numerical analysis of pathway formation of ground water inrush from faults in coal seam floor. China J Rock Mech Eng 28(2):290–297

Li LC, Yang TH, Liang ZZ et al (2011) Numerical investigation of groundwater outbursts near faults in underground coal mines. In J Coal Geol 85:276–288

Liu WT, Wu Q (2008) Numerical simulations of water inrush of fault F0 in Fangezhuang coal mine. Chin J Rock Mech Eng 27(Supp. 2):3604–3610

Lu Y, Wang L (2015) Numerical simulation of mining-induced fracture evolution and water flow in coal seam floor above a confined aquifer. Comput Geotech 67:157–171

Lu HF, Shen D, Yao DX et al (2014) Analytical solution of critical water inrush pressure of mining floor affected by fault. J Min Saf Eng 31(6):888–895

Miao XX, Cui XM, Wang JA et al (2011) The height of fractured water-conducting zone in undermined rock strata. Eng Geol 120:32–39

Peng JB, Chen LW, Huang QB et al (2013) Physical simulation of surface fissures triggered by undersurface fault activity. Eng Geol 155(2):19–30

Qiao W, Hu G, Li WP (2013) Experimental study on the conversion from seepage to flow of water inrush aroused by fault activation in fully mechanized top-coal caving. J Min Saf Eng 30(1):30–37

Shi BQ, Hou ZJ (2011) Mechanical analysis of fault activation water inrush in over burden rock and its application. Rock Soil Mech 32(10):3053–3057

Shi LQ, Xin HQ, Zhai PH et al (2012) Calculating the height of water flowing fracture zone in deep mining. J China Univ Min Technol 41(1):37–41

Song ZQ, Hao J, Tang JQ et al (2013) Study on water inrush from fault's prevention and control theory. J China Coal Soc 38(9):1511–1515

Sun J, Wang LG (2013) Floor fault water-inrush prediction based on catastrophe analysis of micro-seismic signals. J China Coal Soc 38(8):1404–1410

Sun W, Zhou W, Jiao J (2015) Hydro-geological classification and water inrush accidents in China's coal mines. Mine Water Environ 35:214–220

Tang J, Bai H, Bang HY et al (2011) Theoretical analysis on water-inrush mechanism of concealed collapse pillars in floor. Min Sci Technol 21:57–60

Wang C, Zhang N, Han Y et al (2015) Experiment research on overburden mining-induced fracture evolution and its fractal characteristics in ascending mining. Arab J Geosci 8(1):13–21

Wang W, Jiang T, Faybishenko B et al (2016) Closure of fracture due to cover stress re-establishment after coal mining. Geotech Geol Eng 34:1525–1537

Wu Q, Wang M, Wu X (2004) Investigations of groundwater bursting into coal mine seam floors from fault zones. Int J Min Sci Technol 41:557–571

Yin S, Zhang J, Liu D (2015) A study of mine water inrushes by measurements of in situ stress and rock failures. Nat Hazards 79:1961–1979

Yuan R, Li Y, Jiao Z (2015) Movement of overburden stratum and damage evolution of floor stratum during coal mining above aquifers. Proc Eng 102:1857–1866

Zhang H, Cao J, Tu M (2013) Floor stress evolution laws and its effect on stability of floor roadway. Int J Min Sci Technol 23:631–636

Zhang PS, Yan W, Zhang WQ et al (2016) Mechanism of water inrush due to damage of floor and fault activation induced by mining coal seam with fault defects under fluid-solid coupling mode. Chin J Geotech Eng 38(5):877–889

Zhu WB, Wang XZ, Kong X et al (2009) Study of mechanism of stope water inrush caused by water accumulation in over-burden separation areas. Chin J Rock Mech Eng 28(2):306–311

Zhu GL, Zhang WQ, Zhang GB et al (2017) Experimental research on fault activation conducting water inrush. Rock Soi Mech 38(11):3163–3172